Crystallization and Melting Behavior of Polylactides

Jose-Ramon Sarasua,[†] Robert E. Prud'homme,*[,†] Muriel Wisniewski,[‡] Alain Le Borgne,[§] and Nicolas Spassky[‡]

Centre de recherche en sciences et ingénierie de macromolécules and Chemistry Department, Université Laval, Québec, Canada, G1K 7P4, Laboratoire de chimie macromoléculaire, Université Pierre et Marie Curie, 4 place Jussieu, 75252 Paris Cedex 05, France, and Laboratoire de physicochimie des polymères, UMR 27, Université de Paris XII, 2-8 rue Henri-Durant, 94320 Thiais, France

Received October 21, 1997; Revised Manuscript Received March 4, 1998

ABSTRACT: Six polylactides, polymerized with Salen−Al−OCH_3 initiator and having optical purities between 43% and 100%, were analyzed by differential scanning calorimetry, X-ray diffraction, and optical microscopy, following various crystallization conditions. It was found that each of those polylactides can crystallize, even those with low optical purities; their crystallization rate is, however, slower than those for high optical purity polyesters. Moreover, the low optical purity polymers tend to form stereocomplexes between the L and D sequences of the same polylactide, which behavior is ascribed to their multiblock microstructure. A correlation was found between the measured melting temperature of optically active polylactides and their average sequence length.

Introduction

Polylactide is a biodegradable polymer of interest for medical applications such as controlled antibiotic release or fixation of prosthetic joints.[1] Having a chiral center in its molecular structure, polylactide's properties can be varied by forming polymers of different enantiomeric compositions.

Since early works carried out by Fischer et al.,[2] several research groups have studied the crystallization behavior of polylactide and its stereocopolymers. Optically pure polylactide was shown to be a semicrystalline polymer that crystallizes from the melt giving rise to negatively birefringent spherulites.[3] However, as the optical purity of polylactide is lowered, its crystallizability decreases until reaching a threshold composition of 72% beyond which the crystallization is not observed anymore.[4−6]

Isotactic polylactides are prepared from the optically pure monomer because random copolymers are formed from the racemic monomer, as demonstrated by ^{13}C nuclear magnetic resonance (NMR) spectroscopy showing that the polymerization follows a Bernoullian statistics.[7,8] However, some of us[9] have recently reported that the initiator Salen−Al−OCH_3 (resulting from the reaction of a Schiff base on $AlEt_2$ Cl) gives rise to an efficient steric control during the living polymerization of racemic lactides since ^{13}C NMR spectroscopy indicates that long isotactic sequences are preferentially formed. The L/D motif distribution of the chains follows a first-order Markov statistics with a reactivity ratio for the incorporation of L dimer units 2.8 times larger than that of the incorporation of D dimer units.[10,11] In other words, this initiator leads to a sequence distribution of L/D motifs in the polymer backbone that is not random.

In this article, the crystallization from the melt of polylactides prepared using Salen−Al−OCH_3 is studied for optical purities going from 43% to 100%. Differential scanning calorimetry (DSC) experiments are conducted on nascent polymers and thermally treated samples. The morphology of the polymers is studied by optical microscopy and their structure by wide-angle X-ray scattering (WAXS).

The decrease of melting temperature with optical purity is analyzed by the existing theories of copolymer crystallization. Results are compared to those found in random stereocopolymers: it will be shown that the block structure of these polylactides leads to the crystallization of samples of low optical purities.

Table 1. Characteristics of the Stereoregular Polylactides

acronym	$\bar{M}_n$(GPC)	$\bar{M}_n$(NMR)	$\bar{M}_w/\bar{M}_n$	$[\alpha_L^{25}]$ (deg)	o.p. (%)
PLLA100	16800	10100	1.25	−156	100
PLLA80	12600	8850	1.15	−125	80
PLLA70	11500	9500	1.10	−111	71
PLLA60	15800	8550	1.15	−95	61
PLLA50	17000	10600	1.20	−73	47
PLLA40	9550	7050	1.10	−66	43

Experimental Section

The polylactides used in this study were prepared by Wisniewski[11] by ring-opening polymerization with Salen−Al−OCH_3 as initiator, in CH_2Cl_2 at 70 °C. This is a livinglike polymerization process where the secondary reactions of transesterification, which occur in the last stage of the polymerization, were avoided since the polymerization reaction was stopped at 70% of conversion. A detailed description of this synthesis is given in ref 9.

Table 1 shows the number-average molecular weight, the polydispersity index ($\bar{M}_w/\bar{M}_n$), the rotatory power ($[\alpha_L^{25}]$) and the optical purity (o.p.) of these polylactides. Both the number-average ($\bar{M}_n$) and the weight-average ($\bar{M}_w$) molecular weights were determined by gel permeation chromatography (GPC) in tetrahydrofuran using polystyrene standards while $\bar{M}_n$ was also determined by ^1H NMR spectroscopy following the determination of end groups. The rotatory power ($[\alpha_L^{25}]$) was measured in chloroform, at 25 °C, using a concentration of 0.9 g/dL. The optical purity (o.p.) was calculated from

$$\text{o.p.}(\%) = \frac{[\alpha_L^{25}]}{[\alpha_L^{25}]_0} \times 100$$

* To whom correspondence should be addressed. E-mail: Robert.Prud'homme@chm.ulaval.ca.
† Université Laval.
‡ Université Pierre et Marie Curie.
§ Université de Paris XII.

S0024-9297(97)01545-3 CCC: $15.00
Published on Web 05/28/1998

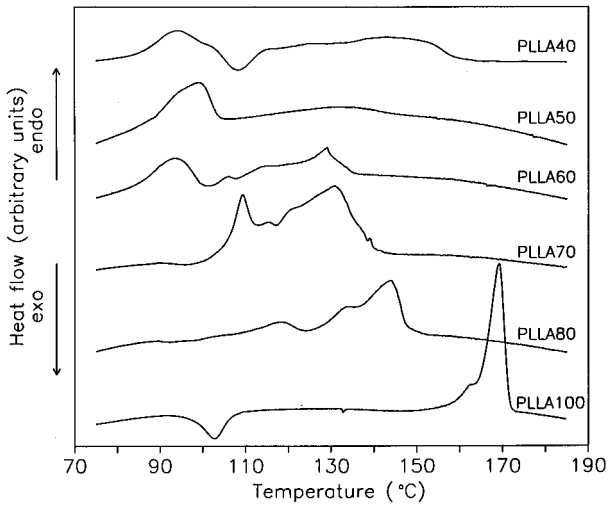

Figure 1. Melting curves of nascent polylactides having optical purities varying from 43% (PLLA40) to 100% (PLLA100). See Table 1 for more details.

where $[\alpha_L^{25}]_0$ is the rotatory power of the optically pure poly(L-lactide). Its value was taken as −156°, the highest experimental rotatory power determined in this study[11] and in ref 16; this value is slightly higher than those of −153 and −150° reported in the literature.[12,13] It is seen that polymers of 43, 47, 61, 71, 80, and 100% optical purity were obtained, hereafter called PLLA40, PLLA50, PLLA60, PLLA70, PLLA80, and PLLA100, respectively.

Differential scanning calorimetry (DSC) measurements were conducted with a Perkin-Elmer DSC-7 apparatus calibrated with pure indium. Several thermal treatments were used as described in the next section of this article. The melting temperature (T_m) was taken at the end of the melting peak. The scan rate was 10 °C/min in all cases, except when indicated otherwise, and the sample size between 8 and 10 mg.

The morphology of each sample was investigated with a Zeiss polarizing microscope equipped with a Mettler FP-5 hot stage. Samples were cooled at 20 °C/min from the melt and, then, isothermally crystallized at 55 °C below their melting point.

X-ray diffraction powder patterns were recorded with a Rigaku Model RU200 X-ray apparatus equipped with a rotating anode generator. Diffraction angles reported are for Cu Kα radiation.

Results and Discussion

Thermal Analysis. Figure 1 shows the thermal behavior of all polylactides investigated. It is seen that each nascent polymer exhibits an endothermic melting peak during the calorimetric scan. PLLA100 gives a small exothermic peak of crystallization at 103 °C, followed by a single endothermic peak (with a shoulder) at 169.2 °C. The thermal behavior of the other polymers is more complex with peaks appearing at lower temperatures as the optical purity is reduced. PLLA80 shows a crystallization exotherm at 124 °C and a double melting peak at 134.5 and 143.9 °C. PLLA70 and PLLA60 also give a double melting peak appearing at 108.4 and 130.7 °C for PLLA70 and at 93.2 and 128.9 °C for PLLA60. Finally, PLLA50 exhibits a single melting peak at 98.9 °C while PLLA40 gives such an irregular shape that no attempt was made to determine T_m and ΔH_m; however, it is clear that this sample exhibits some crystallinity. It is noted that some of the peaks of Figure 1 have an irregular shape; this is found for nascent polymers, which have not been annealed to remove stresses and traces of solvent but not for samples crystallized from the melt, as seen in the following figures.

Table 2. Temperature (T_m) and Enthalpy of Fusion (ΔH_m) of Nascent Polylactides and Temperature (T_c) and Enthalpy of Crystallization (ΔH_c) after Complete Melting

polymer	T_m (°C)[a]	ΔH_m (J/g)[b]	T_c (°C)	ΔH_c (J/g)
PLLA100	174 (169)	61	103	−14
PLLA80	153 (144)	33	124	−2
PLLA70	143 (131)	33		
PLLA60	140 (129)	27		
PLLA50	105 (99)	18		
PLLA40	n.d.[c]	n.d.		

[a] T_m is taken at the end of the high-temperature melting peak. The values in brackets correspond to the maximum of the same endothermic peak. [b] ΔH_m is the sum of the areas under all endothermic peaks. [c] n.d.: the shape of the PLLA40 curve indicates the presence of crystallinity, but it is so irregular that these parameters could not be determined.

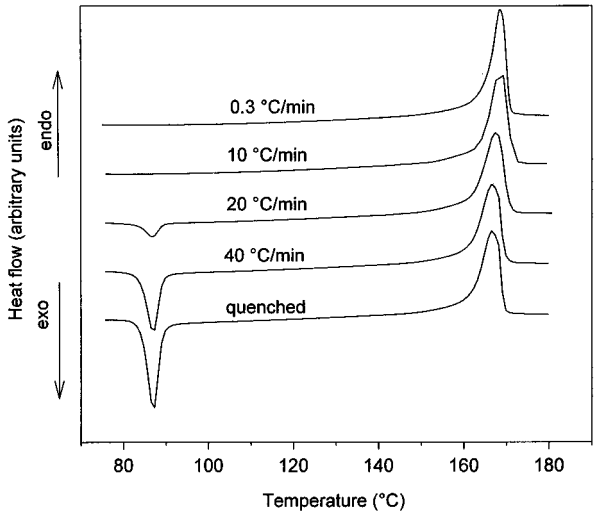

Figure 2. Melting curves of PLLA100, crystallized from the melt at cooling rates between 0.3 and 40 °C/min. The bottom curve was obtained after quenching the sample in the DSC apparatus down to 100 K.

The enthalpies and temperatures of fusion and crystallization of the nascent polylactides are reported in Table 2. It is emphasized that the crystallization of polylactides has been achieved even at low levels of optical purity, although both temperature and enthalpy of fusion decrease with the optical purity. In previous studies on polylactides, it was observed that an optical purity of at least 72% was required for crystallization: 84% by Vert et al.,[4] 78% by Brochu et al.,[5] and 72% by Tsuji and Ikada.[6] Therefore, our results provide evidence of the improved crystallizability of polylactides polymerized with Salen−Al−OCH_3.

The thermal behavior of the polylactides depends highly on the thermal history of the samples. Figures 2 and 3 show the melting curves of PLLA100 and PLLA80, respectively, after cooling from the melt at different rates. In both cases, when the sample is rapidly cooled from the melt, crystallization takes place during the heating scan (at 10 °C/min) giving an exothermic peak at 87 °C for PLLA100 and one at 115 °C for PLLA80. The magnitude of the exotherm decreases when the sample is more slowly cooled, and vanishes at scan rates equal or smaller than 10 °C/min for PLLA100 and at scan rates equal or smaller than 0.3 °C/min for PLLA80.

The corresponding enthalpies of fusion (ΔH_m) and crystallization (ΔH_c) of PLLA100 and PLLA80 are

Table 3. Thermal Properties of Polylactides after Different Thermal Treatments from the Melt

	Thermal Treatment															
	quenching unannealed			40 °C/min unannealed			20 °C/min unannealed			10 °C/min unannealed			0.3 °C/min			
													unannealed		annealed[b]	
polymer	ΔH_c (J/g)	ΔH_m (J/g)	T_m (°C)	ΔH_c (J/g)	ΔH_m (J/g)	T_m (°C)	ΔH_c (J/g)	ΔH_m (J/g)	T_m (°C)	ΔH_c (J/g)	ΔH_m (J/g)	T_m (°C)	ΔH_m (J/g)	T_m (°C)	ΔH_m (J/g)	T_m (°C)
PLLA100	−40	73	170.6	−29	74	172.3	−7	74	172.3		74	174.3	77	174.5	85	181.0
PLLA80	−5	19	147.3	−4	17	147.7	−4	17	148.1	−4	18	147	35	146.5	41	148.9
PLLA70		n.c.[c]			n.c.			n.c.			n.c.		24	141.0	32	138.4
PLLA60		n.c.			n.c.			n.c.			n.c.			n.c.	29	135.0
PLLA50		n.c.			n.c.			n.c.			n.c.			n.c.	19	128.8
PLLA40		n.c.			n.c.			n.c.			n.c.			n.c.	8	121.2

[a] n.c. means no crystallization. [b] Annealing temperature: $T = 105$ °C, $T = 100$ °C, $T = 95$ °C, $T = 90$ °C, $T = 85$ °C, $T = 80$ °C for PLLA100, PLLA80, PLLA70, PLLA60, PLLA50, and PLLA40, respectively; the annealing time was 24 h in each case.

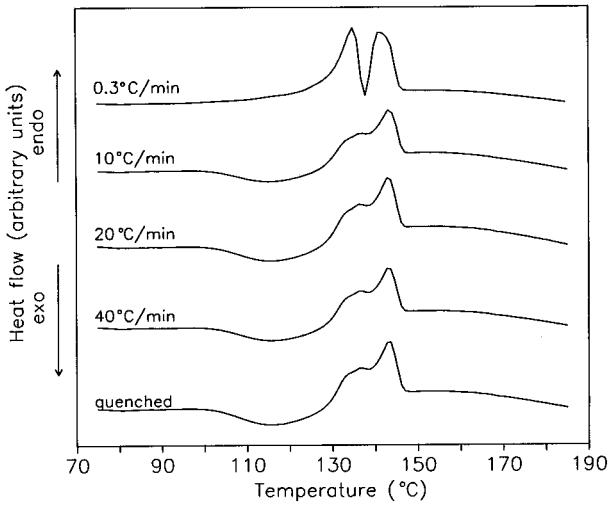

Figure 3. Melting curves of PLLA80 crystallized from the melt at cooling rates between 0.3 and 40 °C/min. The bottom curve was obtained after quenching the sample in the DSC apparatus down to 100 K.

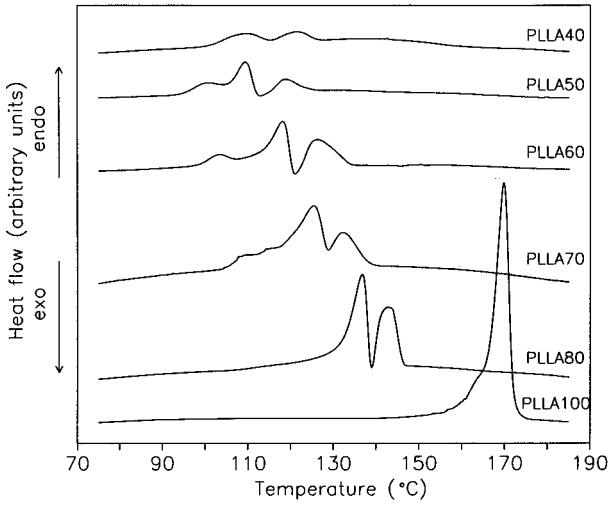

Figure 4. Melting curves of PLLA100, PLLA80, PLLA70, PLLA60, PLLA50, and PLLA40, after a rapid cooling from the melt at 320 °C/min and their isothermal crystallization between 80 and 105 °C (see text).

reported in Table 3. For PLLA100, the melting enthalpy equals about 74 J/g for all conditions, except after annealing where it is higher, at 85 J/g. However, the crystallization is observed under rapid cooling conditions only, and the enthalpy of crystallization increases as the cooling rate goes from 20 to 40 to 320 °C (quenching). This means that the degree of crystallinity of those latter samples at room temperature, after rapid cooling, is smaller than it is after slow cooling (Figure 2). The same trend is observed with PLLA80 whose enthalpy of fusion is close to 18 J/g at intermediate and rapid cooling rates but increases to 35 J/g at a 0.3 °C/min cooling rate and to 41 J/g after annealing. In this case, however, the enthalpy of crystallization remains in the 4−5 J/g range under all conditions, except at 0.3 °C/min where it is not observed.

Table 3 also shows that, after the first melting, the crystallization of polylactides of optical purity lower than 80% is more difficult to achieve. Unlike PLLA100 and PLLA80 that crystallize from the melt under a wide variety of conditions, PLLA70 does not crystallize either when quenched from the melt or when slowly cooled between 40 and 10 °C/min, but it crystallizes when slowly cooled at 0.3 °C/min, with a relatively large enthalpy of fusion of 24 J/g. Moreover, polylactides of lower optical purity require an annealing to crystallize. After annealing, crystallization is achieved for all samples studied with, however, a decrease of melting enthalpy and melting temperature with optical purity. This includes PLLA40, whose crystallization could not be detected during the first DSC scan, reaching a melting enthalpy value of 8 J/g after annealing.

The degree of crystallinity of the samples can be calculated from the ratio of their enthalpy of fusion to the enthalpy of fusion of the polylactide crystal ΔH^0_m. For this purpose, we used a value of 106 J/g for ΔH^0_m.[14] This calculation leads to degrees of crystallinity ranging, for the annealed samples, from 7.6% for PLLA40, to 27% for PLLA60, and to 80% for PLLA100. Smaller ΔH^0_m values of 83−91 J/g[2,3] were reported in the literature as well as higher values of 142−148 J/g.[15−17] Our value, determined by melting point depression analysis, appears reasonable between the two extrema cited.

Figure 4 shows the melting behavior of PLLA100, PLLA80, PLLA70, PLLA60, PLLA50, and PLLA 40, rapidly cooled (320 °C/min) from the melt to 105, 100, 95, 90, 85, and 80 °C, respectively, isothermally crystallized for 24 h, and quenched to 50 °C before the DSC scan. All polylactides, except the optically pure PLLA100 that exhibits a single and sharp melting peak at 181.0 °C, exhibit a complex melting behavior with an exotherm between the two main endotherms.

A double melting peak is a common phenomenon for polymers. It has been observed in poly(ethylene terephthalate),[18−20] isotactic polystyrene,[21−22] poly(ether ether ketone),[23,24] and poly(ether imide),[25] to give just a few examples. It can be due to the presence of two distinct crystal or morphological structures in the initial

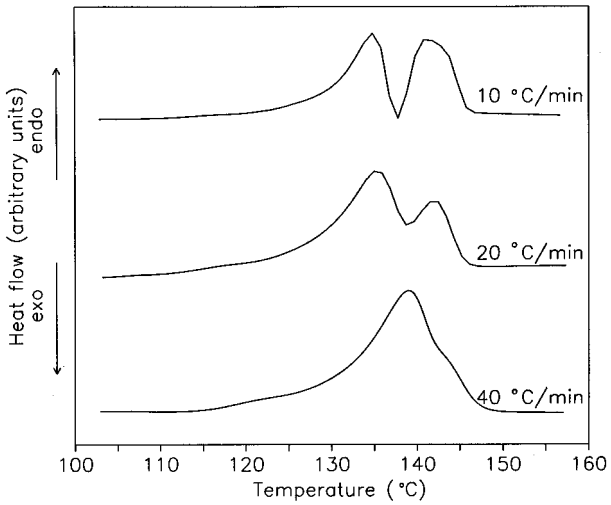

Figure 5. Melting curves of PLLA80 cooled from the melt at 0.3 °C/min and heated at rates of 10, 20, and 40 °C/min.

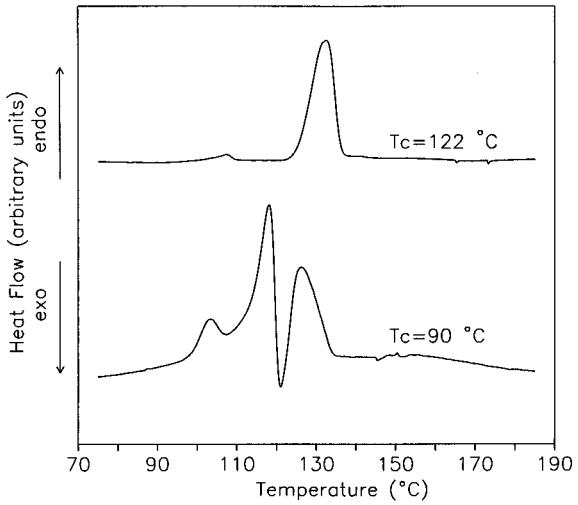

Figure 6. Melting curves of PLLA60 isothermally crystallized at 90 and 122 °C. See text for more details.

sample, but often, it is the result of annealing occurring during the DSC scans whereby crystals of low perfection melt have time to recrystallize a few degrees above and to remelt. To verify this hypothesis, the melting curves of PLLA80 recorded at 10, 20, and 40 °C/min after being slowly cooled from the melt to 95 °C at 0.3 °C/min and quenched to 50 °C are shown in Figure 5. Irrespective of the scanning rate, the melting of PLLA80 occurs between 120 and 150 °C with a constant enthalpy of fusion of 38 J/g. At 10 °C/min, two endotherms of almost equal intensity are observed at 134.5 °C (peak 1) and 141.6 °C (peak 2). When the scan rate is increased to 20 °C/min, the intensity of peak 1 increases relative to that of peak 2, and it is also shifted to higher temperatures by a few degrees. Finally, at 40 °C/min, peak 2 nearly vanishes relative to peak 1 and appears as a shoulder. These results provide evidence of the annealing process described above. When the scan rate is low, i.e., 10 °C/min, there is enough time for the thinner crystals to melt and then to recrystallize before giving a second endotherm at a higher temperature; the area under the higher melting peak corresponds then to the melting of thinner crystals. In contrast, when the scan rate is high, i.e., 40 °C/min, the recrystallization step can hardly occur and the high temperature peak is hardly visible. This evolution as a function of scanning rate is accomplished by a shift of the endotherms to higher temperatures due to a delay of the system, at high scanning rates, to respond. This is the reason, in Figure 5, that peak 1 occurs at 134.5 °C at 10 °C/min but is shifted to 139.0 °C at 40 °C/min, close to the maximum of peak 2 (141.6 °C) at 10 °C/min. These conclusions can be extended to PLLA70, which shows the same qualitative trends as PLLA80 when analyzed as a function of the scanning rate.

This process means that the double melting behavior can be modified if the crystallization occurs isothermally at a relatively high temperature. For example, Figure 6 compares the melting patterns of PLLA60 after crystallizations carried out during 24 h at 90 and 122 °C, then quenched to 50 °C; the latter is the temperature at which a minimum between the two main endotherms is observed for the sample crystallized at 90 °C. As can be observed, PLLA60 crystallized at 90 °C shows a complex melting pattern with two main endotherms located at 135.8 °C and 122.0 °C. In contrast it shows, after crystallization at 122 °C, a single melting endotherm at 140.9 °C since, under these conditions, the recrystallization−melting process cannot occur. Similar observations were made with the other samples exhibiting the double melting behavior (Figure 4), i.e., PLLA40, PLLA50, PLLA70, and PLLA80. In addition to the double melting peak behavior mentioned above, it is noticed in Figures 4−6, that the exotherm is very intense and goes below the baseline. This situation is unusual, but has been observed by others for polylactides,[26] and simply indicates that the crystallization at those temperatures is very rapid.

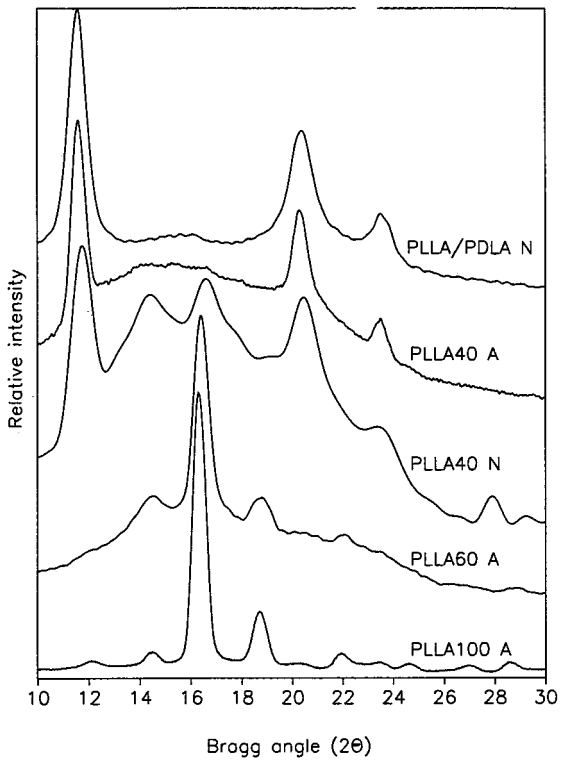

Figure 7. X-ray diffraction curves of PLLA100, PLLA60, PLLA40 (two different crystallization conditions—see text), and of an equimolar mixture of PLLA and PDLA.

Wide-Angle X-ray Scattering (WAXS). Figure 7 shows the X-ray diffraction pattern of PLLA100 (bottom) and of the equimolar mixture (top) of optically pure poly(L-lactide) and poly(D-lactide) (PLLA/PDLA). PLLA100, crystallized 24 h at 120 °C, shows its most intense peaks

at 2θ values of 14.5, 16.3, 18.7, and 21.9°, in agreement with the peaks reported at 15, 16, 18.5, and 22.5° by Ikada et al.[27] for the α form of the optically pure poly(L-lactide) crystallizing in a pseudo-orthorhombic unit cell of dimensions $a = 1.07$ nm, $b = 0.595$ nm, and $c = 2.78$ nm which contains two 10_3 helices[28] (even if the observed diffraction patterns exhibit additional reflections which do not fit a pure 10_3 helix[28−32]). Note that this structure has recently been reduced to a three-chain, trigonal unit cell, and frustrated structure in which the isochiral helices have different setting angles and different environments.[33]

The diffraction pattern of the PLLA/PDLA 50/50 blend is very different from that of PLLA100 since three main diffraction peaks appear at 2θ equal to 12, 21, and 24°. These values are in agreement with the diffraction peaks reported in ref 27. The stereocomplex crystallizes in a triclinic system with the following cell dimensions: $a = 0.916$ nm, $b = 0.916$ nm, $c = 0.870$ nm, $\alpha = 109.2°$, $\beta = 109.2°$, and $\gamma = 109.8°$, in which L-lactide and D-lactide segments are packed parallel taking a 3_1 helical conformation.[28]

Figure 7 also shows the X-ray diffraction patterns of PLLA40 both in its nascent state and after isothermal crystallization from the melt at 111 °C for 24 h and that of PLLA60 crystallized from the melt at 122 °C for 24 h. As expected, PLLA60, like PLLA70 and PLLA80, gives a diffraction pattern that agrees closely with that of PLLA100. However, PLLA40, when crystallized at 111 °C, shows diffraction peaks at 11.6, 20.3, and 23.5°, in agreement with the pattern of the equimolar mixture, leading to the conclusion that the structure of the melt-crystallized PLLA40 is that of the stereocomplex. The diffraction pattern of the nascent polymer of PLLA40 shows, in addition to the three diffraction peaks reported for the stereocomplex, three other peaks at 14.4, 16.6, and 27.9° that closely correspond to the more intense peaks of PLLA100 crystallized in the α form.

Figure 8 shows the X-ray diffraction pattern of PLLA50 in its nascent state and after crystallization from the melt at 113 °C for different annealing times. The nascent PLLA50 exhibits its two more intense peaks at 14.4 and 16.6°, corresponding to the α-crystal form, and peaks of smaller intensity at 11.6, 20.6, and 23.5°, indicating the presence, also, of the stereocomplex form. After melting, however, the diffraction peaks appearing after 12 and 24 h reveal that the stereocomplex develops first, followed at longer annealing times by the development of the α-form crystals.

Figure 9 shows the X-ray diffraction pattern of PLLA50 after a 24 h crystallization from the melt at different temperatures. At 113 and 100 °C, the three characteristic peaks of the stereocomplex are found at 11.6, 20.6, and 23.5°, while the crystallization at 85 °C gives, in addition, three other peaks at 15.6, 16.5, and 18.9°, indicating the simultaneous development of the α-crystal form. The stereocomplex is then more favored at high temperatures of crystallization and the α-form at lower temperatures.

Figure 10 shows the melting behavior of PLLA50 and PLLA 40 when crystallized for 24 h at 90 and 85 °C and also at the temperature corresponding to the minimum between the double endotherm of Figure 4, i.e., 113 °C for PLLA50 and 111 °C for PLLA40. As for PLLA60, the multiple melting peak found at 85 or 90 °C becomes a quasi-single peak after crystallization at 111 or 113 °C, and this peak is shifted to higher

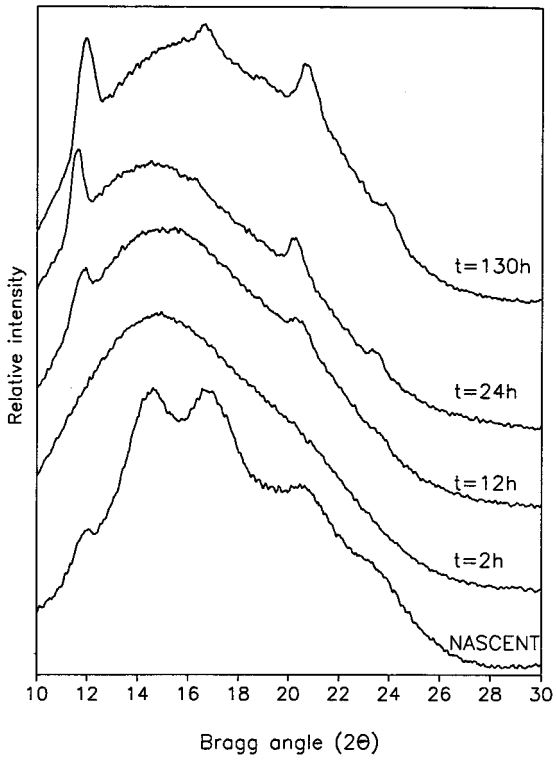

Figure 8. X-ray diffraction curves of PLLA50 in its nascent state, and crystallized at 113 °C between 2 and 130 h.

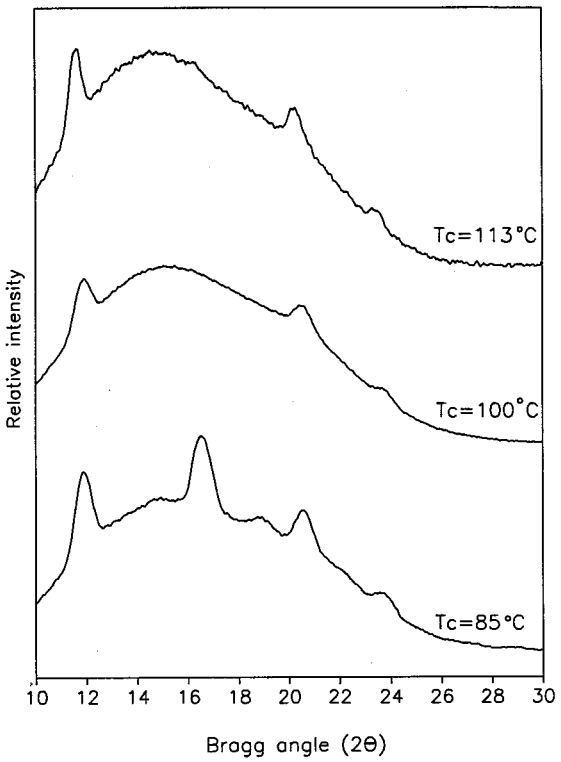

Figure 9. X-ray diffraction curves of PLLA50 crystallized isothermally at 85, 100, and 113 °C for 24 h.

temperatures. In both cases, a second peak of smaller intensity is also observed at higher temperatures than the principal peak. Figure 10 shows the thermogram of the equimolar mixture of the optically pure PLLA/PDLA, with a melting temperature of 253 °C, 78 °C higher than that shown by the nascent PLLA100. Indeed, when a stereocomplex is formed between species of similar chemical structure, an increase in the melting

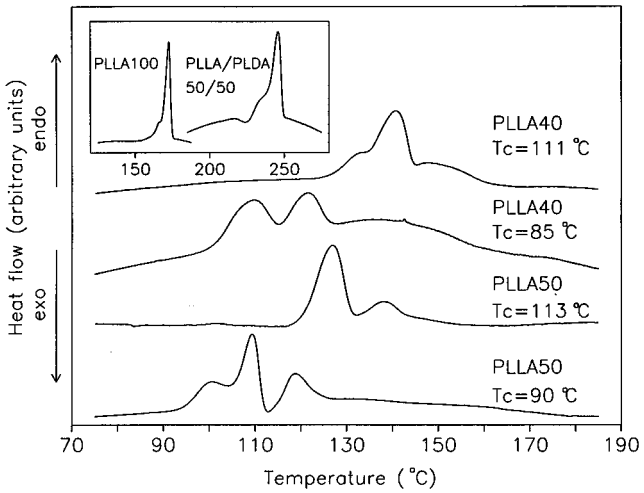

Figure 10. Melting curves of PLLA50 crystallized isothermally at 90 and 113 °C and of PLLA40 crystallized isothermally at 85 and 111 °C. The insert gives, as a reference, the melting curves of pure PLLA100 and a 50/50 mixture of PLLA100 and PLDA100.

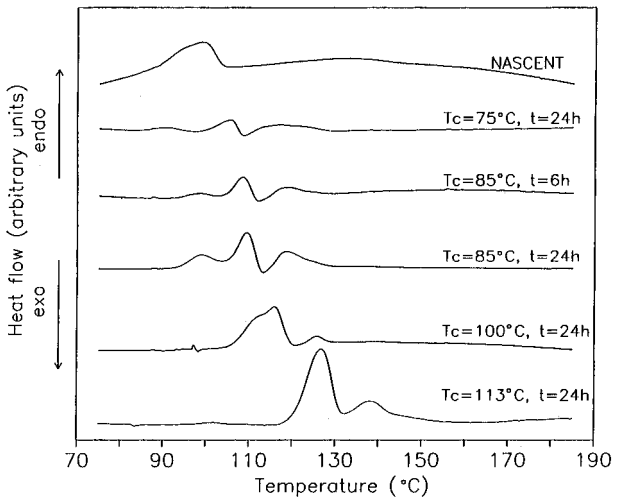

Figure 11. Melting curves of PLLA50 isothermally crystallized from the melt between 75 and 113 °C. The top curve was obtained for the nascent polymer.

temperature can be observed; for example, for both the optically active forms of poly(*tert*-butyl thiirane)[34] and poly (α-methyl-α-ethyl-*β*-propiolactone),[35] the stereocomplex was found to melt at approximately 40 °C above either of its enantiomeric component. For the polylactides, the stereocomplex formed of enantiomerically pure species[5,6,12] has been reported to melt at 50 °C above its pure components whereas when one of components of the stereocomplex has an optical purity of 80%, the melting temperature is only 25 °C higher than that of the pure components.[5]

Figure 11 shows the DSC curves of PLLA50 crystallized from the melt at different temperatures. The samples crystallized at 113 and 100 °C give a double melting peak that, on the basis of the X-ray diffraction patterns of Figure 9, can be attributed to the stereocomplex. The samples crystallized at 75 and 85 °C show similar shapes with three endotherms centered at 91.0, 105.4, and 117.1 °C in the first case and at 98.0, 108.4, and 120.0 °C in the second case. In addition, a small exotherm is also observed at 109.2, 111.2, and 113.2 °C, for samples crystallized at 75, 85 (6 h), and 85 °C (24 h), respectively. As revealed by the diffraction patterns of Figure 9, two different crystal structures coexist after crystallization at these temperatures. Since spherulites of the α-form of PLLA50 crystallized at 85 °C were found to melt at 115 °C (see the next section about the morphology), it seems that the high-temperature endotherm represents the melting of the stereocomplex crystals whereas the low-temperature double endotherm represents the melting of the α-crystals. The presence of a small intermediate exotherm suggests the recrystallization of some of the α-crystals into the stereocomplex structure during the scan.

The correlation between the intensity of the diffraction peaks for each structure developed in the nascent PLLA50 of Figure 8 with the enthalpies of fusion calculated for each of its endotherms in Figure 1 also indicates that nascent PLLA50 crystallizes basically in the α-form, giving a relatively intense endotherm peak at 98.9 °C, as compared to the small endotherm at higher temperatures corresponding to the melting of the stereocomplex. However, X-ray and DSC data of the nascent PLLA40 of Figures 8 and 1, respectively, point to an increase in the population of the stereocomplex vs the α-form crystals as compared to those found in PLLA50.

Morphology. Figure 12 shows the morphology of PLLA100, PLLA80, PLLA70, PLLA60, PLLA50, and PLLA40 crystallized from the melt at 120, 95, 90, 80, 75, and 75 °C, respectively, i.e., at about $T_m - 55$ °C. All polymers studied here, irrespective of the enantiomeric composition, show a spherulitic morphology. PLLA100 gives a narrow distribution of sizes, with an average radius of 117 μm. The average size of the spherulites decreases with optical purity; it goes to 9 μm for PLLA80, to 5 μm for PLLA70, and to 2 μm for PLLA60. However, PLLA50 shows somewhat larger spherulites of 10 μm while PLLA40 gives, in addition to these spherulites, spots of low birefringence that are due to the presence of spherulites of very small sizes (<1 μm).

Figure 13 shows the two different spherulitic morphologies found in PLLA50 crystalized at 113 °C. First, there is a large population of small spherulites of about 5 μm that are randomly distributed in the micrographs; second, in addition to the predominant spherulites, two highly birefringent spherulites of larger size (∼75 μm) are also observed in specific areas (Figure 13a). When the temperature is increased, at 3 °C/min, to 125 °C, these two spherulites begin to lose some of their birefringence (Figure 13b) until 128 °C where they have been extinguished (Figure 13c). Since the spherulites of smaller size do not melt until 143 °C, they can be associated to stereocomplex crystals, while the larger spherulites having a lower melting point grow from the α-form crystal. These results agree with the X-ray diffraction patterns of Figure 9 in which it was observed that PLLA50 crystallized at 113 °C gives the stereocomplex crystal structure, with some α-crystals which develop at long annealing times.

Figure 14 finally shows the evolution of the crystal morphology of PLLA50 as a function of temperature. At 113 °C, PLLA50 gives stereocomplex spherulites of 5 μm in radius (Figure 14a). At 100 °C, small birefringent spherulites of about 1 μm in radius can also be observed, but in specific areas, like the one shown in Figure 14b, there are also some large α-spherulites. At 85 °C, PLLA50 gives well-defined spherulites with an average radius of about 70 μm (smaller than at 100 °C,

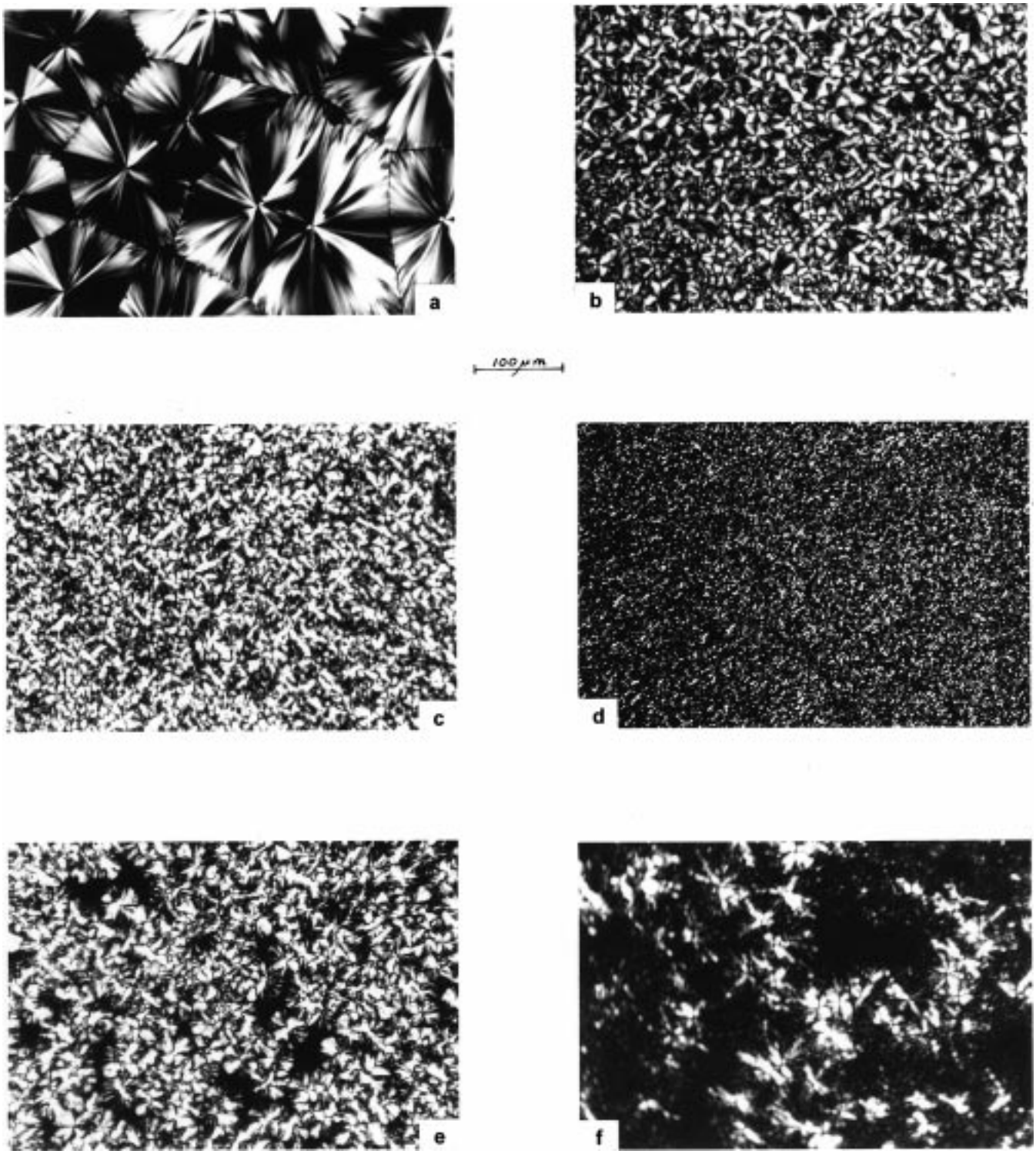

Figure 12. Optical photomicrographs (between crossed polars) of samples isothermally crystallized from the melt. See text for details: (a) PLA100; (b) PLLA80; (c) PLLA70; (d) PLLA60; (e) PLLA50; (f) PLLA40. In all cases, the crystallization was pursued long enough that no further change could be detected under the polarizing microscope.

Figure 14b), that melt completely at 115 °C. From the X-ray data of Figure 10 and the DSC data of Figure 11, these spherulites, larger in size for this composition than expected from Figure 12, are attributed to the α form. Therefore, morphological studies also indicate, in addition to the X-ray and DSC results, for PLLA50, a progressive transition in the crystal structure from that of the stereocomplex to that of the α-form, as the crystallization temperature decreases. Finally, Figure 14d shows the same sample as in Figure 14c when the crystallization is completed, i.e., when the spherulites are volume filling.

Discussion

Figure 15 shows the melting temperature of the annealed polylactides of Table 1 (prepared with Salen−Al−OCH_3) as a function of optical purity. For comparison, the melting temperature of polylactides prepared from other initiators is also given: powdered zinc,[4] Al-

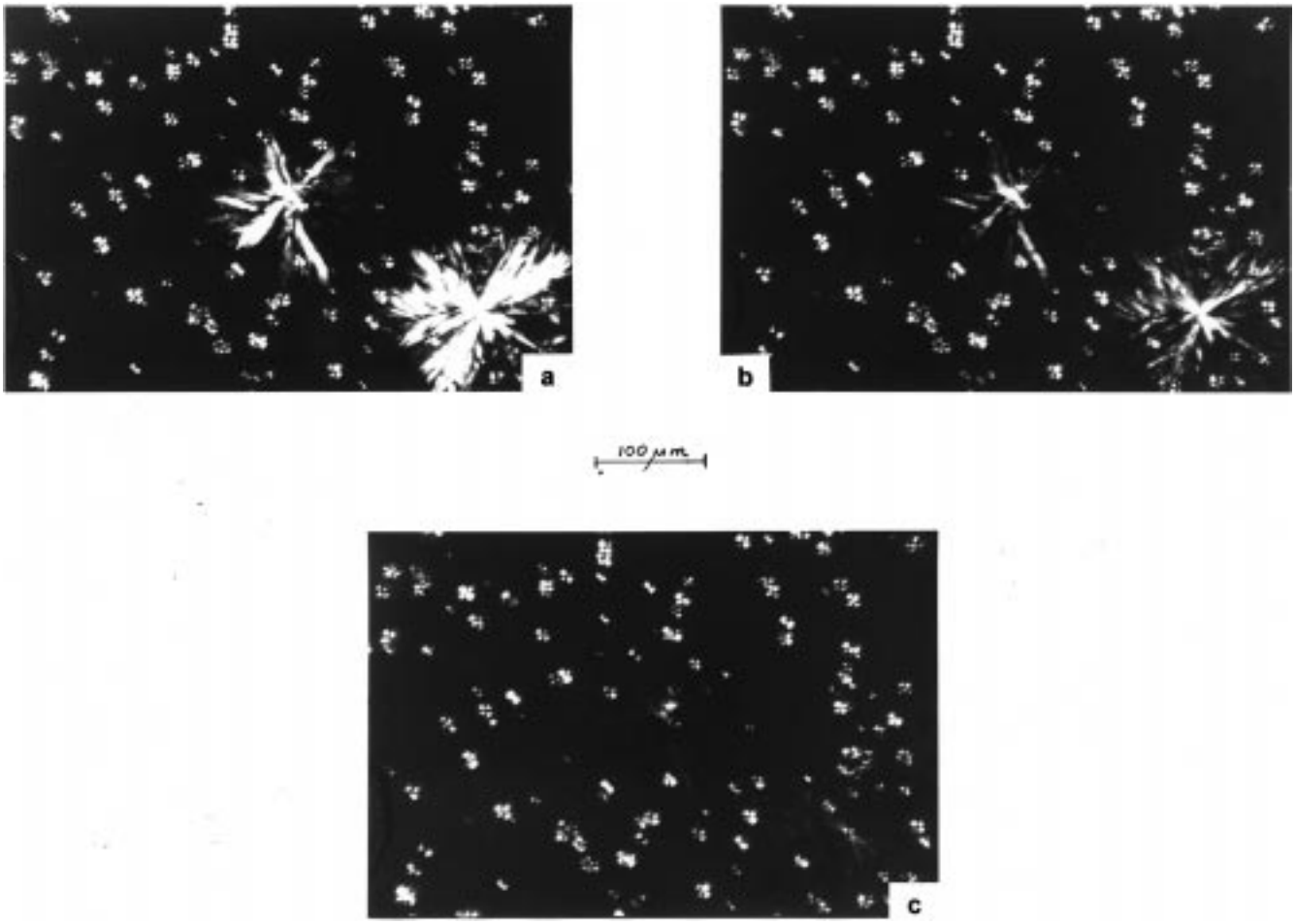

Figure 13. Optical photomicrographs (between crossed polars) of PLLA50 crystallized at 113 °C. The pictures were taken: (a) at room temperature; (b) at 125 °C; (c) at 128 °C.

$(OiPr)_3$,[5] and lauryl alcohol.[6] It is again seen that polylactides obtained with Salen−Al−OCH_3 crystallize at optical purities lower than those required in other series. However, the melting point depression is of the same order in each series of samples since the lowest melting temperature recorded is here 121.2 °C as compared to 122, 133, and 129 °C in refs 4, 5, and 6, respectively. For comparison, the values calculated using Flory's eq 36 are also represented. This theory, which is a total exclusion theory, reads

$$\Delta H_m^0 \left(\frac{1}{T_m} - \frac{1}{T_m^0} \right) = -R \ln X_L \qquad (1)$$

where T_m is the melting temperature of the copolymer, T_m^0 the melting temperature of the pure polymer, ΔH_m^0 the enthalpy of fusion, X_L the molar fraction of crystallizable L units, and R the gas constant. Here, X_L is calculated from the enantiomeric excess of the polymer which is taken equal to the experimentally measured optical purity; T_m^0 is taken equal to 454 K, the melting temperature of PLLA100 after annealing; and $\Delta H_m^0 = 10.7$ kJ/mol (see the previous section). At each composition, the calculated values from eq 1 exceed the experimental values. There are two main reasons why Flory's theory fails to predict correctly the experimental data. First, it considers a random copolymer microstructure. Second, it does not take into account a partial inclusion of the comotif.[35,36] We will come back later on these points. Let us note, however, that eq 1 predicts the equilibrium melting points of the copolymers whereas the experimental values given in Figure 15 are not.

The microstructure of these polylactides was studied by solution ^{13}C NMR spectroscopy and their tetrad distributions determined.[9] This experimental distribution was found in agreement with the distribution calculated with a first-order Markov statistics[10] and a reactivity ratio of 2.8. This result indicates the preferential formation of isotactic sequences, contrary to other initiators[4−6] that give a random distribution of D and L units in the chain.

Figure 16 illustrates the structure of a polymer chain of enantiomeric excess of 30%. Case a corresponds to a Bernoullian distribution of motifs, whereas case b results from a first-order Markov statistics with $r = 2.8$. For comparison, the stereoblock structure is also shown (case c). The increase in the number-average length of the isotactic sequences ($\bar{L}$) of L and D motifs, as the microstructure goes from random to Markov, indicates the tendency of the growing chain to add a unit of the same kind as the terminal unit for a given initial optical purity. In each case, $\bar{L}$ can be calculated by the Mayo−Lewis equation[39,40]

$$\bar{L} = 2(1 + rp) \qquad (2)$$

where $p = X_L/X_D$ is the molar ratio of the two enantiomers and r is the reactivity ratio. When $r = 1$, the

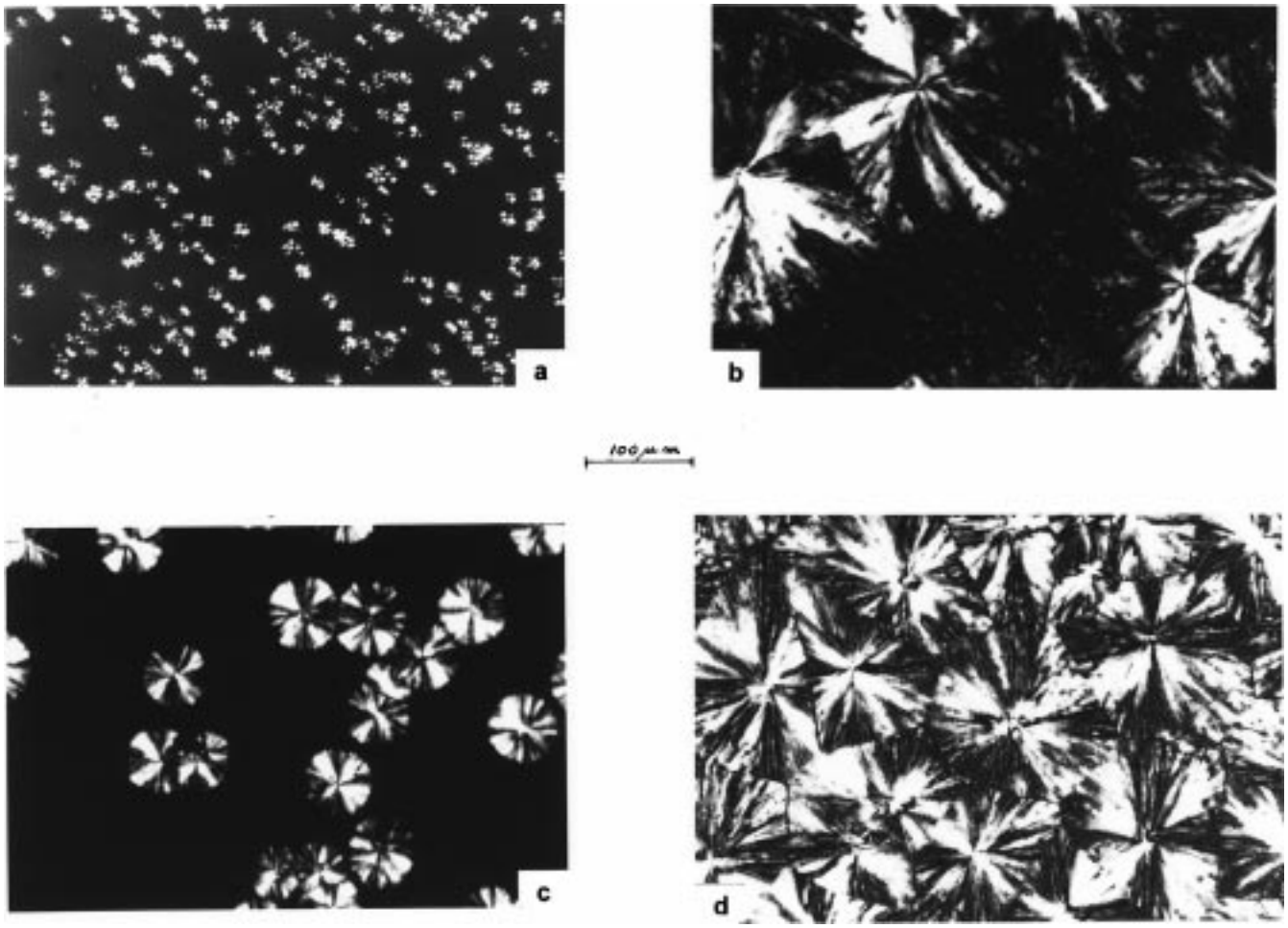

Figure 14. Optical photomicrographs (between crossed polars) of PLLA50 crystallized at (a) 113 °C, (b) 100 °C, and (c and d) 85 °C. Picture c depicts the sample in the course of crystallization, and picture d shows the sample after completion of the crystallization.

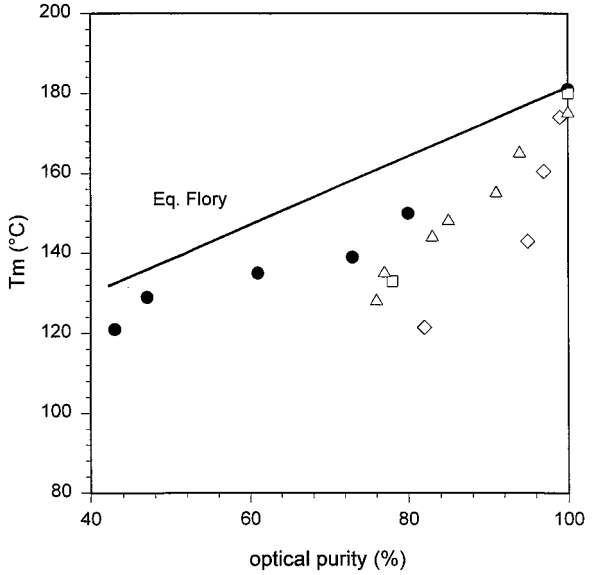

Figure 15. Melting temperatures of several series of polylactides as a function of optical purity: this work (●); ref 4 (◇); ref 5 (□); and ref 6 (△).

condition for having statistical copolymers, eq 2, reduces to

$$\bar{L} = 2/X_D \tag{3}$$

A factor of 2 is introduced in both equations to take into account that the addition of lactide units goes in pairs.[11]

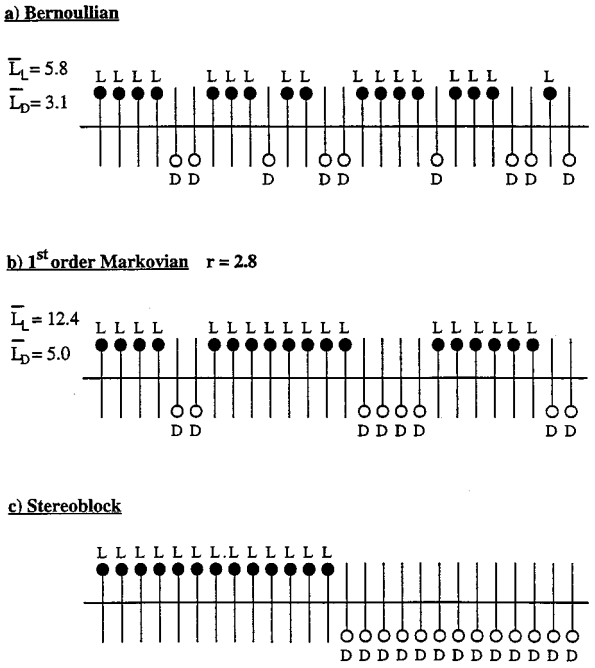

Figure 16. Schematic representation of (a) Bernoullian, (b) Markovian, and (c) stereoblock microstructures.

Table 4 shows $\bar{L}$ values calculated for each polylactide. For the fully isotactic optically pure poly(L-lactide), a

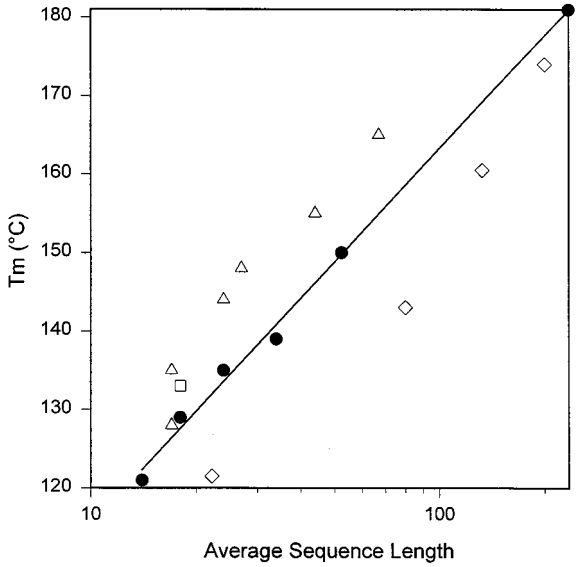

Figure 17. Melting temperatures of the polylactides shown in Figure 15 as a function of their calculated sequence length. The same symbols were used as in Figure 15.

Table 4. Number Average Isotactic Sequence Length ($\bar{L}$) and Effective Number Average Isotactic Sequence Length ($\bar{L}^e$) of Polylactides

polymer	Bernoulli	first order Markov
PLLA100	234	234
PLLA80	20.0	52
PLLA70	13.3	34
PLLA60	10.0	24
PLLA50	7.7	18
PLLA40	7.0	14

value of 234 was calculated from its GPC molecular weight (Table 1). $\bar{L}$ decreases with optical purity, and for each composition, Markovian structures show longer sequences than Bernoullian structures. The polylactide of lower optical purity considered here, PLLA40, has a value of 14, in agreement with a variety of ethylene copolymers in which block lengths between 5 and 15 repeat units were considered necessary to observe crystallization.[41−45] However, if there is a partial inclusion of D units into the L-crystals, which is probable in view of the multiblock structure of the samples,[9,10] the L crystallizing sequence length in those polylactides is longer than that reported in Table 4. This value of 14 is in excellent agreement with the value of 15 recently reported by Tsuji and Ikada[46] for random copolymers of D and L-lactides, corresponding however to an optical purity of 76%, as compared to 43% in this work for PLLA40. These values are smaller that the 40 units required in L-lactide ϵ-caprolactone copolymers.[47]

Taking into account the average sequence lengths calculated in Table 4 for the Salen−Al−OCH_3 series of polylactides and doing a similar calculation for the other data points given in Figure 15, which are random copolymers (i.e., $r = 1$ in eq 2), we obtained the melting temperatures plotted in Figure 17 as a function of $\bar{L}$. A reasonable correlation is now obtained indicating that the average sequence length of the enantiomeric L unit is the controlling variable of the crystallization of polylactides. Taking into account this factor, all series of polylactides behave similarly. So far, no polylactide has been found to be able to crystallize for an average sequence length below 14 (Figure 17).

Conclusions

The multiblock microstructure of polylactides prepared with the Salen−Al−OCH_3 initiator leads to their crystallization, even with optical purities as low as 40%, as compared to a "low" limit of 70−80% in the literature for samples prepared by more classical initiators[4−6,46]. An interesting consequence of this microstructure is that stereocomplexes are formed between the L and D blocks of the same chains, intramolecularly or intermolecularly, as shown by the X-ray diffraction patterns of samples of optical purities of 40, 50, and 60%. We did not detect any sign of these stereocomplexes with polylactides of optical purities of 80% or 70%.

Acknowledgment. The authors thank the Natural Sciences and Engineering Research Council of Canada (NSERCC) and the Department of Education of Québec for supporting this work.

References and Notes

(1) Zhang, X.; Goosen M. F. A.; Wyss U. P.; Pichora, D. *J. Macromol. Sci. Rev. Macromol. Chem. Phys.* **1993**, *C33*, 81.
(2) Fischer, E. W.; Sterzel,; Wegner, H. J. *Kolloid-Z. Z. Polym.* **1973**, *251*, 980.
(3) Kalb, B.; Pennings, A. J. *Polymer* **1980**, *21*, 607.
(4) Vert, M.; Chabot, F.; LeRay, J.; Christel, P. *Macromol. Chem. Suppl.* **1981**, *Suppl. 5*, 30.
(5) Brochu, S.; Prud'homme R. E.; Barakat I.; Jérôme R. *Macromolecules* **1995**, *28*, 8, 5230.
(6) Tsuji, H.; Ikada, Y. *Macromolecules* **1992**, *25*, 5719.
(7) Chabot F.; Vert M.; Chapelle S.; Granger P. *Polymer* **1983**, *24*, 53.
(8) Bero, M.; Kasperczyk, J.; Jedlinski, Z. *Makrommol. Chem.* **1990**, *191*, 2287.
(9) Wisniewski, M.; Le Borgne, A.; Spassky, N. *Makrom. Chem. Phys.* **1997**, *198*, 1227.
(10) Le Borgne, A.; Spassky, N.; Jun, C. L.; Momtaz, A. *Makromol. Chem.* **1988**, *189*, 637.
(11) Wisniewski, M. Ph.D. Thesis, Université Pierre et Marie Curie (Paris VI), 1995.
(12) Yui, N.; Dijkstra, P. J.; Feijen, J. *Makromol. Chem.* **1990**, *191*, 481.
(13) Tonelli, A. E.; Flory, P. J. *Macromolecules* **1969**, *2*, 225.
(14) Caron, J. F. M.Sc. Thesis, Laval University **1996**.
(15) Cohn, D.; Younes, H., Marom, G. *Polymer* **1987**, *28*, 2018.
(16) Gilding, D. K.; Reed, A. M. *Polymer* **1979**, *20*, 1459.
(17) Loomis, G. L.; Murdoch, J. R.; Gardner, K. H. *Polym. Prepr.* **1990**, *39* (2), 55.
(18) Holdsworth, P.; Turner-Jones, A. *Polymer* **1971**, *12*, 195.
(19) Alfonso, G. C.; Pedemonte, E.; Ponzetti, L. *Polymer* **1979**, *20*, 104.
(20) Roberts, R. C. *Polymer* **1969**, *10*, 117.
(21) Lemstra, P. J.; Kooistra, T.; Challa, G. J. *J. Polym. Sci., Polym. Phys. Ed.* **1972**, *10*, 823.
(22) Boon, J.; Challa, G.; van Krevelen, D. W. *J. Polym. Sci., Polym. Phys. Ed.* **1968**, *6*, 1791.
(23) Lee, Y.; Porter, R. S. *Macromolecules* **1987**, *20*, 1336.
(24) Blundell, D. J. *Polymer* **1987**, *28*, 2248.
(25) Brandom D. K.; Wilkes G. L. *Polymer* **1995**, *35*, 5672.
(26) Bélorgey, G. Private communication.
(27) Ikada, Y.; Jamshidi, K.; Tsuji, H.; Hyon, S. H. *Macromolecules* **1987**, *20*, 906.
(28) Okihara, T.; Tsuji, M.; Kawaguchi, A.; Katayama, K. I.; Tsuji, H.; Hyon, S. H.; Ikada, Y. *J. Macromol. Sci.—Phys.* **1991**, *B30* (1&2), 119.
(29) De Santis, P.; Kovacs, A. J. *Biopolymers* **1968**, 6, 299.
(30) Eling, B.; Gogolewski, S.; Pennings, A. *J. Polymer* **1982**, *23*, 1587.
(31) Hoogsteen, W., Postema, A. R.; Pennings, A. J.; ten Brinke, G.; Zugenmaier, P. *Macromolecules* **1990**, *23*, 634.
(32) Brizzolara, D.; Cantow, H. J.; Diedericks, K.; Keller, E.; Domb, A. J. *Macromolecules* **1996**, *29*, 191.
(33) Cartier, L.; Spassky, N.; Lotz, B. *C. R. Acad. Sci., Paris, Ser. 2b* **1996**, *322*, 429.
(34) Dumas, P.; Spassky, N.; Sigwalt, P. *Makromol. Chem.* **1972**, *156*, 55.
(35) Grenier, D.; Prud'homme, R. E. *J. Polym. Sci., Polym. Phys. Ed.* **1984**, *22*, 577.

(36) Flory, P. J. *Trans. Faraday Soc.* **1955**, *51*, 848.
(37) Helfand, E.; Lauritzen, J. I., Jr. *Macromolecules* **1973**, *6*, 631.
(38) Sanchez, I. C.; Eby, R. K. *Macromolecules* **1987**, *20*, 906.
(39) Mayo, F. R.; Lewis, F. M. *J. Am. Chem. Soc.* **1944**, *66*, 1594.
(40) Coleman M. M.; Varnell, W. D. *J. Chem. Educ.* **1975**, *59*, 847.
(41) Killian, H. G. *Kolloid Z. Z. Polym.* **1963**, *189*, 23.
(42) Jackson, J. F. *J. Polym. Sci., Part A* **1963**, *1*, 2119.
(43) Krigas, T. M.; Carella, J. M.; Struglinsky, M. J.; Crist, B.; Graessley, W. W. *J. Polym. Sci., Polym. Phys. Ed.* **1985**, *23*, 509.
(44) Bowmer, T. N.; Tonelli, A. E. *J. Polym. Sci. Polym. Phys. Ed.* **1986**, *24*, 1631.
(45) Burfield, D. R. *Macromolecules* **1987**, *20*, 3020.
(46) Tsuji, H.; Ikada, Y. *Makrom. Chem. Phys.* **1996**, *197*, 3483.
(47) Stevels, W. M.; Ankoné, M. J. K.; Dijkstra, P. J.; Feijen, J. *Makrom. Chem. Phys.* **1995**, *196*, 1153.

MA971545P